
PURE AND MIXED DICKE STATE ANSATZ FOR EQUALITY AND INEQUALITY CONSTRAINTS IN VARIATIONAL QUANTUM EIGENSOLVER

✉ J.V.S Scursulim

josevictor.s.scursulim@gmail.com

June 9, 2026

ABSTRACT

Combinatorial optimization can be addressed with quantum computing through variational quantum algorithms, but a central challenge in this approach is to design an ansatz expressive enough to explore the feasible subspace of the Hilbert space where the optimal solution lies. Another major challenge is tuning the Lagrange multipliers in penalty terms to enforce feasibility and guarantee solution quality. To address both challenges, we propose the first feasibility-preserving mixed Dicke state ansatz for Hamming weight constrained combinatorial optimization, extending the density matrix formalism to structurally encode equality and inequality constraints directly into the quantum circuit, thereby eliminating the need for penalty terms in the objective function. The proposed framework handles both constraint types, with the pure Dicke state ansatz recovered as a special case corresponding to equality constraints, and generalizes to multiple constraint groups via tensor products of individual pure or mixed Dicke states. We validate the proposed approach in the context of combinatorial portfolio optimization across three experimental scenarios with increasing constraint complexity, using the CMA-ES optimizer and comparing its performance against random search with replacement restricted to the feasible subspace. As the feasible search space grows, the proposed ansatz demonstrates a clear advantage over random search in terms of the number of objective function calls required to identify high-quality solutions. Hardware experiments on IBM NISQ processors confirm that noise mitigation and circuit transpilation optimizations remain open challenges for practical deployment. The framework is general and directly applicable to other combinatorial optimization problems with Hamming weight constraints.

Keywords Variational Quantum Eigensolver · Dicke State · Density Matrix · Combinatorial Optimization · Inequality Constraints · Equality Constraints

I Introduction

Quantum computing is an emerging technology that offers potential computational advantages over classical computing for specific problem classes. This computing paradigm is based on the principles of quantum mechanics, where phenomena such as superposition, entanglement, relative phase, and interference are used as computational resources to achieve gains in algorithmic complexity [1, 2, 3, 4, 5]. In the near term, noisy quantum hardware devices, combined with error mitigation techniques, can yield computationally relevant results. In the long term, fault-tolerant quantum computers are expected to deliver significant advances in physics [6, 7, 8, 9, 10], chemistry [11, 12, 13, 14, 15, 16], combinatorial optimization [17, 18, 19, 20, 21, 22, 23, 24], machine learning [25, 26, 27, 28, 29, 30, 31, 32] and finance [33, 34, 35, 36, 37].

Combinatorial optimization arises in numerous problems of practical relevance across research, industry, and business, including the traveling salesman problem, portfolio optimization, tail assignment, facility location, Birkhoff decomposition, and others. These problems can be addressed with classical techniques such as mixed-integer programming and metaheuristics. However, as the number of variables and constraints scales, the computational cost of finding

optimal solutions grows exponentially, often rendering exact methods intractable or forcing solvers to return suboptimal approximations within practical time limits.

Currently available quantum processors, while comprising hundreds to thousands of physical qubits, remain susceptible to noise, limiting their applicability to large-scale problems due to gate errors, decoherence, and limited qubit connectivity [38]. A promising near-term strategy combines error mitigation techniques [39, 40, 41, 42, 43, 44, 45, 46, 47, 48], optimization problem decomposition [49], and variational quantum algorithms (VQAs) [50]. Two of the most studied VQAs are the Variational Quantum Eigensolver (VQE) [51] and the Quantum Approximate Optimization Algorithm (QAOA) [52], both of which alternate between parameterized quantum circuits and classical optimization routines. Even in the noise-free regime, VQAs face fundamental challenges that hinder the achievement of practical quantum advantage, including ansatz expressivity [53], barren plateaus [54, 55], finite sampling noise [56], and classical parameter optimization [57].

In this work, we propose the first feasibility-preserving mixed Dicke state ansatz for Hamming weight constrained combinatorial optimization, extending the density matrix formalism and open quantum systems theory [58, 59] — previously explored in broader VQA contexts [60, 61, 62, 63] — to the domain of structured combinatorial optimization with equality and inequality constraints. We provide a theoretical framework alongside experimental results that validate the proposed approach in the context of portfolio optimization. The framework is general and directly applicable to other combinatorial optimization problems with Hamming weight constraints, such as feature selection and ensemble selection [64, 65].

This manuscript is organized as follows. Section II presents the combinatorial optimization problems addressed in this work. Section III discusses the theoretical aspects of the proposed ansatz. Section IV describes the experimental settings. Sections V and VI present the experimental results and discuss the findings in light of the theoretical framework. Section VII provides the concluding remarks and directions for future work. Complementary discussions are presented in the Appendix.

II Combinatorial Portfolio Optimization

Modern portfolio theory [66] provides a theoretical foundation for portfolio construction by balancing expected return and risk. In combinatorial portfolio optimization, the goal is to select a subset of assets that maximizes the expected return while minimizing risk. The mathematical formulation of this problem is given by the mean-variance model

$$\min_{x \in \{0,1\}^n} qx^T \Sigma x - (1 - q)x^T \mu + r_f, \quad (1)$$

where x is the binary decision variable vector, Σ is the covariance matrix, μ is the vector of expected asset returns, $q \in [0, 1]$ is the risk aversion factor that incorporates investor preferences, r_f is the risk-free return, often approximated by the interest rate of the US Treasury. Since r_f is a constant, it does not affect the optimal solution and is typically omitted in practice.

Beyond the objective function, constraints play a central role in portfolio optimization by encoding regulatory requirements, risk limits, and structural preferences. In combinatorial portfolio optimization, a natural constraint is to impose an upper bound, a lower bound, or an exact value on the Hamming weight of the decision variables, which in financial terms determines the number of assets selected to compose the portfolio. Such constraints are modeled mathematically as follows:

$$\sum_i x_i = b \quad (2)$$

$$\sum_i x_i \leq b \quad (3)$$

$$\sum_i x_i \geq b. \quad (4)$$

Since $b \in \mathbb{N}$, strict inequality constraints can be rewritten as non-strict ones by replacing b by $b + 1$ and $b - 1$ in equations (3) and (4) respectively. In practice, multiple constraints of the forms (2), (3), and (4) can be combined to encode diversification requirements, generating more robust portfolios as highlighted in [37].

III VQE with Pure and Mixed Dicke State Ansatz

Quantum computing addresses combinatorial optimization problems through the isomorphism between Quadratic Unconstrained Binary Optimization (QUBO) and Ising models, recasting the optimization problem as a ground state

energy search. The optimization problem can be cast as a QUBO following the procedures described in [67], and through the change of variables $x_i = \frac{1-Z_i}{2}$ [68], the QUBO is converted into an Ising Hamiltonian that encodes the original problem. Quantum mechanics guarantees the existence of a ground state for physically valid Hamiltonians; however, finding this ground state exactly is generally intractable. Fortunately, the variational principle [69] provides a mathematical framework to approximate the ground state energy: one proposes a parameterized trial wavefunction, commonly referred to as an ansatz, to evaluate the Hamiltonian expectation value. Inspired by the variational principle, the VQE algorithm combines a parameterized quantum circuit and a classical optimizer to minimize the Hamiltonian expectation value through the following objective function

$$\min_{\vec{\theta} \in \mathbb{R}^d} \langle \psi(\vec{\theta}) | H | \psi(\vec{\theta}) \rangle. \quad (5)$$

Parameterized quantum circuits are composed of rotation and entangling gates, but designing a circuit structure with sufficient expressivity to minimize (5) is generally a nontrivial task. However, structured optimization problems provide information that can be embedded directly into the ansatz: constraints of the forms (2), (3), and (4) restrict the Hamming weight of the decision variables, suggesting that a quantum state designed to satisfy this property by construction is a natural ansatz choice — the Dicke state being the canonical example. The Dicke state originates from a physical model describing the interaction between light and matter [70], and has since been studied in the context of quantum networks [71], quantum metrology [72], quantum error correction [73], and quantum storage [74]. Recent work has further proposed resource-efficient heralded schemes for their preparation in linear-optical platforms [75], broadening the prospects for practical implementation in quantum technologies.

In [37, 76], a pure parameterized Dicke state is proposed as an ansatz for VQE to solve combinatorial portfolio optimization with the equality constraint (2). This parameterized quantum state is given by

$$|D_k^n(\vec{\theta})\rangle = \sum_i \mathcal{P}_i c_i(\vec{\theta}) |0\rangle^{\otimes(n-k)} \otimes |1\rangle^k, \quad (6)$$

where $c_i(\vec{\theta})$ is the probability amplitude and \mathcal{P}_i denotes the i -th permutation operator acting on computational basis states with Hamming weight k . Substituting $|\psi(\vec{\theta})\rangle$ in (5) with (6) using a Hamming weight k that matches the equality constraint, the penalty term can be eliminated by setting its associated Lagrange multiplier to zero. Furthermore, (6) defines a feasible search space whose size grows as $O(n^k)$. When $n \gg k$, this feasible subspace is exponentially smaller than the full search space of size $O(2^n)$, resulting in a significant reduction in the complexity of the optimization landscape.

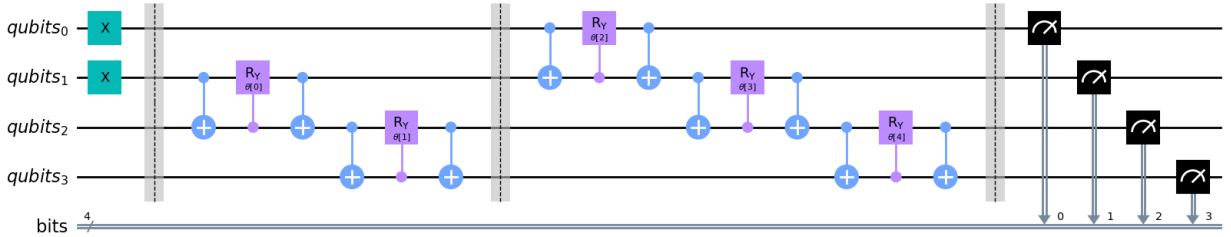


Figure 1: An example of a quantum circuit that generates a pure Dicke state ansatz for VQE. In this figure, the circuit shown prepares the parameterized quantum state $|D_2^4(\vec{\theta})\rangle$.

Inequality constraints (3) and (4) are satisfied by any Dicke state $|D_k^n\rangle$ whose Hamming weight satisfies $k \leq b$ and $k \geq b$, respectively. A quantum state encoding a superposition over such Dicke states can be written as

$$|\phi(\vec{\alpha}, \vec{\theta})\rangle = \sum_k \sqrt{p_k(\vec{\alpha})} |D_k^n(\vec{\theta})\rangle_A \otimes |k\rangle_B, \quad (7)$$

where subsystem B , represented by $|k\rangle_B$ consists of ancilla qubits added to the quantum circuit to control the conditional preparation of each Dicke state.

Density matrices provide a general framework for describing both ensembles of quantum states and the dynamics of open quantum systems [58, 77, 59, 78]. To construct an ansatz that generates an ensemble of Dicke states, we consider the density matrix obtained from the outer product of (7):

$$\begin{aligned} \rho_{AB}(\vec{\alpha}, \vec{\theta}) &= |\phi(\vec{\alpha}, \vec{\theta})\rangle \langle \phi(\vec{\alpha}, \vec{\theta})| \\ &= \sum_{k,l} \sqrt{p_k(\vec{\alpha})} \sqrt{p_l(\vec{\alpha})} |D_k^n(\vec{\theta})\rangle \langle D_l^n(\vec{\theta})| \otimes |k\rangle \langle l|. \end{aligned} \quad (8)$$

Tracing the degrees of freedom of the subsystem B from 8, we obtain the reduced density matrix

$$\begin{aligned}\sigma(\vec{\alpha}, \vec{\theta}) &= \text{tr}_B(\rho_{AB}) \\ &= \sum_k p_k(\vec{\alpha}) |D_k^n(\vec{\theta})\rangle \langle D_k^n(\vec{\theta})|,\end{aligned}\quad (9)$$

which describes a mixture of Dicke states with different Hamming weight values, where $p_k(\vec{\alpha})$ dictates the probability of preparing $|D_k^n(\vec{\theta})\rangle$. Figure 2 shows an example of a quantum circuit that produces the mixture described by (9). Note that the ancilla qubit represents subsystem B in (7), and that the measurement gates implement the partial trace operation.

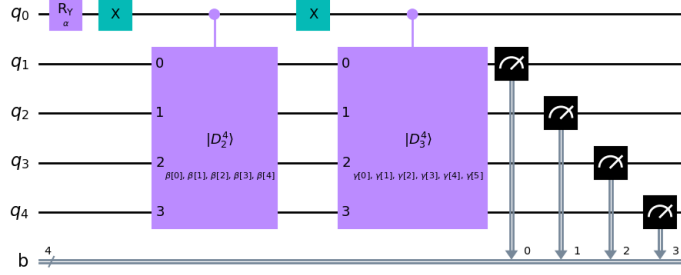


Figure 2: An example of a quantum circuit that creates a mixture of Dicke states as an ansatz for VQE. In this figure, the circuit shown creates a mixture of two quantum states, $|D_2^4(\vec{\beta})\rangle$ and $|D_3^4(\vec{\gamma})\rangle$, where the preparation probability of each state is regulated by the parameterized rotation gate $R_Y(\alpha)$. Note that the measurements only acts on the qubits where Dicke states are prepared, then they can be interpreted as a partial trace and providing us a mixture of quantum states.

In the density matrix formalism, the expectation value of an operator O is given by $\langle O \rangle = \text{tr}(\rho O)$ [58, 77, 59, 78], where ρ is the density matrix of the system. Accordingly, the VQE objective function generalizes to

$$\min_{\vec{\alpha}, \vec{\theta} \in \mathbb{R}^d} \text{tr}(\sigma(\vec{\alpha}, \vec{\theta})H). \quad (10)$$

Note that when $\sigma = |\psi(\vec{\theta})\rangle \langle \psi(\vec{\theta})|$ is a pure state, (10) reduces to (5). For combinatorial optimization problems mapped into an Ising model, the Hamiltonian is diagonal, $H = \sum_{x \in \{0,1\}^n} E_x |x\rangle \langle x|$, the equation (10) reduces to

$$\min_{\vec{\alpha}, \vec{\theta} \in \mathbb{R}^d} \sum_m \sigma_{mm}(\vec{\alpha}, \vec{\theta}) E_m, \quad (11)$$

where $\sigma_{mm}(\vec{\alpha}, \vec{\theta})$ are the diagonal terms of the density matrix $\sigma(\vec{\alpha}, \vec{\theta})$, corresponding to the probability distribution over the computational basis states obtained from measurements on the quantum circuit. For a detailed derivation of (10), the reader is referred to Appendix A.

The framework introduced above naturally extends to optimization problems with multiple Hamming weight constraints by exploiting the tensor product structure of composite quantum systems. Consider C groups of n_c decision variables, where group c is subject to a constraint of the form (2), (3), or (4) with bound b_c . The global ansatz is then given by the tensor product of the individual mixtures

$$\sigma(\vec{\alpha}, \vec{\theta}) = \bigotimes_{c=1}^C \sigma_c(\vec{\alpha}_c, \vec{\theta}_c) = \bigotimes_{c=1}^C \sum_{k_c} p_{k_c}(\vec{\alpha}_c) |D_{k_c}^{n_c}(\vec{\theta}_c)\rangle \langle D_{k_c}^{n_c}(\vec{\theta}_c)|, \quad (12)$$

where each subsystem has its own parameter vectors $\vec{\alpha}_c$ and $\vec{\theta}_c$. This construction satisfies all constraints simultaneously by design, without requiring penalty terms. Furthermore, it subsumes the pure state ansatz of [37] as a special case, recovered when each mixture σ_c collapses to a single Dicke state with fixed Hamming weight $k_c = b_c$. This formulation also accommodates mixed constraint types within the same problem: subsystems subject to equality constraints (2) are represented by pure Dicke states with fixed Hamming weight $k_c = b_c$, while subsystems subject to inequality constraints (3) or (4) are represented by genuine mixtures over the feasible range of Hamming weights.

The number of variational parameters in the ansatz is directly related to the number of constraints, the number of qubits, and the Hamming weight bounds. The total parameter count of the quantum circuit is given by

$$n_p = \sum_{i=1}^s \sum_{k=k_{min,i}}^{k_{max,i}} kn_i - \frac{k(k+1)}{2} + \sum_{i=1}^s (k_{max,i} - k_{min,i}), \quad (13)$$

where s is the number of constraint groups, and $k_{min,i}$ and $k_{max,i}$ are the Hamming weight lower and upper bounds for the i -th group. Note that for equality constraints, where $k_{min,i} = k_{max,i}$, the ancilla term vanishes and the expression reduces to the parameter count of a single pure Dicke state ansatz for each constraint group, consistent with [37].

Although the experimental validation in this work focuses on portfolio optimization, the proposed ansatz is applicable to any combinatorial optimization problem whose feasibility conditions can be expressed as equality or inequality constraints on the Hamming weight of the decision variables, such as feature selection [64] and ensemble selection [65]

IV Methods

To evaluate the effectiveness of the proposed ansatz, we design three experimental scenarios. In all scenarios, the case $k = 0$, corresponding to an empty portfolio with no assets selected, is excluded from the feasible set by setting the lower bound of each mixture to $k_{min} \geq 1$, as it has no financial relevance. The size of the feasible search space is computed by $\sum_k C_{n,k}$ single-group scenarios, where $C_{n,k} = n!/k!(n-k)!$ is the binomial coefficient, and as $\prod_i \sum_{k_i} C_{n_i, k_i}$ for multi-group scenarios involving tensor product ansatz.

Scenario I consists of a portfolio optimization with 11 assets subject to the inequality constraint $k \leq 4$, requiring two ancilla qubits to prepare the mixture

$$\sigma_I(\vec{\alpha}, \vec{\theta}) = \sum_{k=1}^4 p_k(\vec{\alpha}) |D_k^{11}(\vec{\theta})\rangle \langle D_k^{11}(\vec{\theta})|. \quad (14)$$

The feasible search space for this scenario has size $|\mathcal{F}_I| = \sum_{k=1}^4 C_{11,k} = 561$. Scenario II extends the previous one by introducing two simultaneous inequality constraints, $k \geq 3$ and $k \leq 6$, so that the ansatz becomes

$$\sigma_{II}(\vec{\alpha}, \vec{\theta}) = \sum_{k=3}^6 p_k(\vec{\alpha}) |D_k^{11}(\vec{\theta})\rangle \langle D_k^{11}(\vec{\theta})|. \quad (15)$$

The feasible search space for this scenario has size $|\mathcal{F}_{II}| = \sum_{k=3}^6 C_{11,k} = 1419$. Scenario III was designed to validate the tensor product construction and to test a setting combining equality and inequality constraints. We construct a portfolio optimization instance by randomly selecting assets from 4 sectors of the S&P 500 index — Energy, Financial Services, Real Estate, and Basic Materials — with 5 assets per sector. The constraints were defined as follows: an equality constraint $k_E = 3$ for Energy, two inequality constraints $1 \leq k_{FS} \leq 2$ for Financial Services, an equality constraint $k_{RE} = 2$ for Real Estate, and two inequality constraints $1 \leq k_{BM} \leq 4$ for Basic Materials. To prepare the ansatz, 3 ancilla qubits were added, yielding the following tensor product mixture

$$\sigma_{III}(\vec{\alpha}, \vec{\theta}) = \sigma_E \otimes \sigma_{RE} \otimes \sigma_{FS} \otimes \sigma_{BM}. \quad (16)$$

where each subsystem density matrix is defined as

$$\sigma_E = |D_3^5(\vec{\theta})\rangle \langle D_3^5(\vec{\theta})|, \quad \sigma_{RE} = |D_2^5(\vec{\theta})\rangle \langle D_2^5(\vec{\theta})|, \quad (17)$$

$$\sigma_{FS} = \sum_{k_{FS}=1}^2 p_{k_{FS}}(\vec{\alpha}) |D_{k_{FS}}^5(\vec{\theta})\rangle \langle D_{k_{FS}}^5(\vec{\theta})|, \quad \sigma_{BM} = \sum_{k_{BM}=1}^4 p_{k_{BM}}(\vec{\alpha}) |D_{k_{BM}}^5(\vec{\theta})\rangle \langle D_{k_{BM}}^5(\vec{\theta})|. \quad (18)$$

The feasible search space for this scenario has size $|\mathcal{F}_{III}| = \prod_i \sum_{k_i} C_{n_i, k_i} = 45000$.

The CMA-ES optimizer [79] was selected as the primary optimizer based on its performance in [37] and because it is gradient-free, as further discussed in Appendix B. Experiments were also conducted with COBYLA [80] for comparison purposes; however, given its substantially lower success rate in preliminary analysis, the main results focus on CMA-ES. In all experiments, we evaluated 2^i shots for $i \in \{0, 1, \dots, 12\}$ and a maximum number of iterations of 10^j for $j \in \{0, 1, 2, 3\}$. For each scenario, 100 independent experiments were conducted for each combination of shots and iterations, each initialized from a distinct randomly generated initial point, with the random seed fixed to 42 for reproducibility.

All simulations were performed on a personal workstation running Ubuntu 24.04.4 LTS, equipped with an AMD Ryzen 9 9950X3D processor (16 cores, 32 threads) and 64 GB of DDR5 RAM clocked at 6400 MHz. The first two experimental scenarios were simulated using the CPU, while the third scenario, due to its larger scale, required GPU acceleration and was executed on an NVIDIA GeForce RTX 4080 Super with 16 GB of VRAM. All code was developed in Python 3.11, making use of the following packages: NumPy, Matplotlib, Seaborn, Pandas, SciPy, pylatexenc, Qiskit [81], Qiskit IBM Runtime, Qiskit Aer GPU (CUDA 11), ipynb, Plotly, Qiskit Addon Optimization Mapper, CPLEX, Gurobi, CMA-ES [79], Optuna, yfinance, tqdm, nbformat, and Qiskit Experiments. The complete computational environment, including package versions and Python interpreter, is specified in a Pipfile available in the project repository (see Code Availability statement).

V Results

This section presents the simulation results. As mentioned in Section IV, experiments were performed with both CMA-ES and COBYLA. However, due to COBYLA’s constraints on setting a maximum number of iterations and its substantially lower success rate in preliminary analysis, we focus on CMA-ES results. Our goal is not to determine which optimizer performs best, but to validate the proposed framework. Interestingly, in the few cases where COBYLA successfully identified the optimal solution, the resulting distribution was nearly concentrated on the target bitstring, suggesting that its primary limitation in this setting is robustness to finite sampling noise rather than convergence quality.

Figures 3 and 4 present the main simulation results. Figure 3 shows the probability of finding the optimal solution as a function of the number of objective function calls for all three scenarios, compared against random search with replacement restricted to the feasible subspace. Figure 4 shows the portfolios sampled in the best performing experiment for each scenario, positioned relative to the classical efficient frontier.

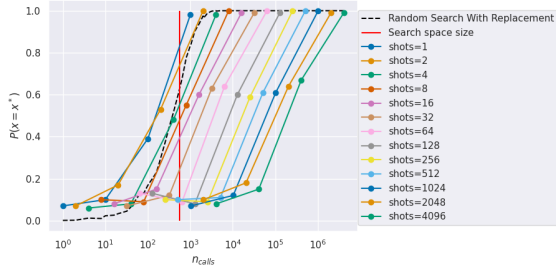
Figure 3 shows the probability of finding the optimal solution $P(x = x^*)$ as a function of the number of objective function calls n_{calls} , comparing the VQE-Dicke framework against random search with replacement restricted to the feasible subspace. As the feasible search space size increases from Scenario I to Scenario III, the advantage of VQE-Dicke over random search becomes more pronounced, as the optimization process progressively concentrates probability mass toward the optimal solution. This behavior is consistent with the theoretical argument that the proposed ansatz is most effective in the regime where the feasible search space is large enough to make exhaustive random sampling impractical. All CMA-ES and COBYLA results for each scenario and experimental setting described in Section IV are available in the project repository (see Data Availability statement).

Figure 4 illustrates how the bitstrings sampled from the optimized distribution can be used to analyze the quality of feasible solutions in the context of portfolio optimization. These results highlight that even when the optimizer fails to drive the reduced density matrix to fully concentrate on the optimal bitstring x^* , the sampled bitstrings still provide a set of high-quality feasible solutions that can be further analyzed or used as warm starts for classical post-processing.

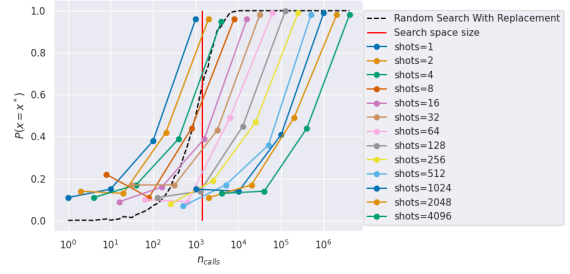
VI Discussion

The results presented in Section V demonstrate that the VQE-Dicke framework successfully identifies optimal or near-optimal portfolio solutions across all three experimental scenarios, with a clear advantage over random search with replacement as the feasible search space grows. In this section, we discuss the theoretical and practical implications of these findings. We first analyze the computational complexity of the proposed framework and the reduction of the feasible search space afforded by the ansatz construction. We then discuss the ideal convergence behavior of the optimization process and the practical strategy for extracting high-quality solutions from the sampled distribution. Finally, we address the impact of hardware noise on the proposed ansatz, with particular attention to bit-flip and readout errors, and discuss the robustness properties of the mixed Dicke state ansatz in the presence of such noise.

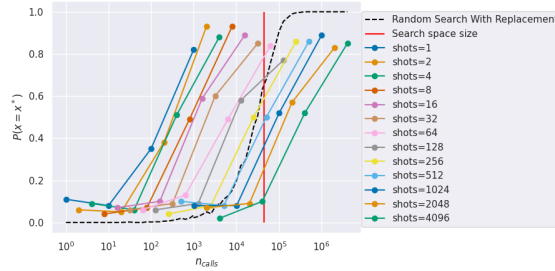
The computational complexity of VQE scales as $\mathcal{O}(N_{iter} \times N_{shots} \times N_{gcp})$, where N_{gcp} is the number of groups of commuting Pauli operators required to estimate the Hamiltonian expectation value. For combinatorial optimization problems mapped into an Ising model, the Hamiltonian is diagonal and all its terms commute, yielding $N_{gcp} = 1$ and thereby reducing the complexity to $\mathcal{O}(N_{iter} \times N_{shots})$. Furthermore, the ansatz defined by (6) and (9) satisfy constraints (2), (3), and (4) by construction, reducing the search space from $\mathcal{O}(2^n)$, which includes infeasible solutions, to the feasible subspace of size $\mathcal{O}(n^k)$, which is exponentially smaller than $\mathcal{O}(2^n)$ in the regime $n \gg k$. For problems with multiple constraints, the feasible search space is dominated by $\mathcal{O}(n^{k_{max}})$, which remains exponentially smaller than $\mathcal{O}(2^n)$, under the assumption $n \gg k_{max}$.



(a) Scenario I

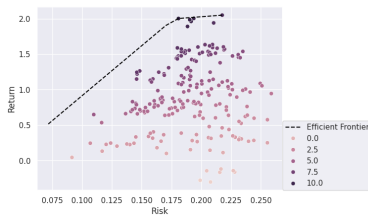


(b) Scenario II

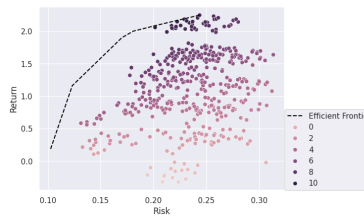


(c) Scenario III

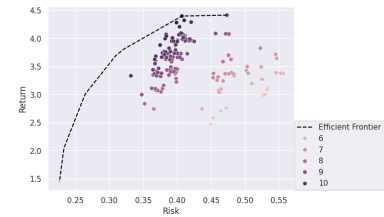
Figure 3: Probability of finding the optimal solution $P(x = x^*)$ as a function of the number of objective function calls n_{calls} for Scenarios I (left, $|\mathcal{F}_I| = 561$), II (center, $|\mathcal{F}_{II}| = 1419$), and III (right, $|\mathcal{F}_{III}| = 45000$), using the CMA-ES optimizer. Each curve corresponds to a different number of measurement shots, and each point represents the empirical success probability estimated over 100 independent runs, where success is defined as the optimal bitstring x^* having non-zero sampling probability after training with the corresponding number of objective function calls. The dashed black curve shows the expected performance of random search with replacement restricted to the feasible search space, and the vertical red line indicates the feasible search space size $|\mathcal{F}|$. Curves crossing the red line to the left indicate configurations where the proposed ansatz outperforms random search in terms of the number of objective function calls. The advantage over random search becomes more pronounced as the feasible search space size increases from Scenario I to Scenario III.



(a) Scenario I



(b) Scenario II



(c) Scenario III

Figure 4: Discrete efficient frontier for Scenarios I (left), II (center), and III (right), showing portfolios sampled from the experiment in which the target bitstring x^* was observed with the highest sampling probability after training, selected among 100 independent runs per scenario. Each point represents a feasible portfolio, colored by Sharpe ratio. The dashed line indicates the discrete efficient frontier computed via classical mean-variance optimization. In all three scenarios, the proposed ansatz successfully identifies portfolios on or near the efficient frontier.

Considering that $\vec{\alpha}^*$ and $\vec{\theta}^*$ are the optimal parameter vectors and x^* is the optimal solution, the ideal behavior of the ansatz after optimization is for the reduced density matrix to converge to

$$\sigma(\vec{\alpha}^*, \vec{\theta}^*) = |x^*\rangle\langle x^*|, \quad (19)$$

corresponding to a distribution concentrated entirely on the optimal bitstring x^* . In the continuous analogy, this is equivalent to a Dirac delta distribution $\delta(x - x^*)$ centered at x^* , which in the discrete setting becomes a Kronecker delta δ_{x,x^*} over the feasible search space. Achieving this ideal behavior, however, may require a large number of optimizer iterations and circuit evaluations, potentially exceeding the feasible search space size $|\mathcal{F}|$ and performing worse than random search with replacement in terms of the number of objective function calls, as discussed in [56]. In practice, a more pragmatic strategy is to sample the optimized circuit and analyze the most frequently observed bitstrings, selecting the one that yields the lowest objective function value. This approach leverages the fact that, even when $\sigma(\vec{\alpha}^*, \vec{\theta}^*)$ does not fully collapse to $|x^*\rangle\langle x^*|$, the optimization process tends to concentrate probability mass around high-quality solutions, making the most frequent bitstrings strong candidates for the optimal or near-optimal solution. As illustrated in Figure 4, the bitstrings sampled from the optimized distribution can be mapped onto the risk-return space and compared against the classical efficient frontier, providing a practical tool for portfolio analysis even in cases where perfect convergence is not achieved.

Finally, it is important to discuss the impact of hardware noise on the proposed ansatz when considering its execution on real quantum devices. The results obtained through real quantum devices will be discussed in more detail in the Appendix C. Quantum states defined by (6) and (9), due to their characteristic Hamming weight structure, are particularly sensitive to bit-flip and readout errors, since these errors can alter the Hamming weight of each state in the superposition. The bit-flip channel acting on a single-qubit density matrix ρ is modeled by [58, 77, 59]

$$\mathcal{E}(\rho) = (1 - p)\rho + pX\rho X. \quad (20)$$

It is worth noting that the proposed ansatz circuit relies heavily on two-qubit gates for the conditional preparation of each Dicke state block, and two-qubit gate errors are typically the dominant source of noise in superconducting quantum hardware [6, 82]. A more realistic error model would therefore consider a two-qubit bit-flip channel acting on each pair of interacting qubits [58, 77, 59]

$$\mathcal{E}_{ij}(\rho) = (1 - p)^2\rho + p(1 - p)(X_i\rho X_i + X_j\rho X_j) + p^2 X_i X_j \rho X_i X_j, \quad (21)$$

where p is the error probability per two-qubit gate, and i, j denote the qubit indices involved in each gate. The evolution of the parameterized mixed state (9) under two-qubit bit-flip channels acting on all interacting qubit pairs in the circuit is given by

$$\sigma'(\vec{\alpha}, \vec{\theta}) = \bigotimes_{(i,j) \in \mathcal{G}} \mathcal{E}_{ij}(\sigma(\vec{\alpha}, \vec{\theta})), \quad (22)$$

where \mathcal{G} denotes the set of interacting qubit pairs defined by the circuit connectivity, and \mathcal{E}_{ij} denotes the two-qubit bit-flip channel acting on qubits i and j . In the case of (6), a single bit-flip is sufficient to corrupt the Hamming weight and displace the state outside the feasible set. For (9), however, only states at the boundary of the feasible range, i.e. those with $k = k_{min}$ or $k = k_{max}$, can be displaced outside the feasible set by a single bit-flip, whereas multiple simultaneous bit-flips can compromise interior states as well. This implies that (9) exhibits greater robustness to single bit-flip errors compared to (6), as the mixture over multiple Hamming weight values preserves a larger portion of the feasible search space. Nevertheless, both error types impact the objective functions (5) and (10), potentially degrading the optimization process. It is therefore important to employ error mitigation techniques targeting readout and bit-flip errors when executing this ansatz on quantum hardware, so as to preserve the Hamming weight structure of the prepared states.

VII Conclusion

In this work, we introduced a variational quantum optimization framework that leverages pure and mixed Dicke states to structurally encode both equality and inequality constraints directly into the quantum circuit ansatz. By operating within the density matrix formalism and applying partial traces via ancilla measurements, we eliminated the need for penalty terms and Lagrange multiplier tuning in the objective function.

Our experimental validation on combinatorial portfolio optimization across three distinct constraint settings — including a complex multi-sector setup utilizing tensor product mixtures — demonstrated that the proposed ansatz can significantly outperform random sampling restricted to the feasible search space in terms of objective function calls. Furthermore, optimization runs successfully mapped assets onto or near the classical efficient frontier. Hardware implementations

on IBM NISQ processors highlighted the inherent trade-offs: while the ansatz exhibits greater theoretical robustness to single bit-flip errors affecting boundary states, it remains sensitive to cumulative two-qubit gate noise, yielding a relative error of approximately 50% across QPUs.

Future work will investigate the integration of advanced error mitigation techniques, such as zero-noise extrapolation or probabilistic error cancellation, combined with circuit transpilation optimizations, to reduce the performance gap between simulation and hardware execution. The proposed framework is general and directly applicable to other combinatorial optimization problems with Hamming weight constraints, such as feature selection and ensemble selection, opening promising directions for further experimental validation.

Disclaimer

This work is purely academic. The portfolio optimization problem is used solely as a benchmark for combinatorial optimization methods and does not constitute financial advice or investment recommendations.

Data availability

The data used in this study are publicly available through Yahoo Finance API and can also be obtained using scripts available in the following GitHub repository: <https://github.com/jvscursulim/quantum-optimization-dicke-states>. The dataset covers the period 05/05/2025 to 05/04/2025 and asset identifiers have been anonymized.

Code availability

All code developed during this research is publicly available in the following GitHub repository: <https://github.com/jvscursulim/quantum-optimization-dicke-states>.

References

- [1] David Deutsch and Richard Jozsa. Rapid solution of problems by quantum computation. *Proceedings of the Royal Society of London. Series A: Mathematical and Physical Sciences*, 439(1907):553–558, 1992.
- [2] Ethan Bernstein and Umesh Vazirani. Quantum complexity theory. In *Proceedings of the twenty-fifth annual ACM symposium on Theory of computing*, pages 11–20, 1993.
- [3] Peter W Shor. Algorithms for quantum computation: discrete logarithms and factoring. In *Proceedings 35th annual symposium on foundations of computer science*, pages 124–134. Ieee, 1994.
- [4] Lov K Grover. A fast quantum mechanical algorithm for database search. In *Proceedings of the twenty-eighth annual ACM symposium on Theory of computing*, pages 212–219, 1996.
- [5] Aram W Harrow, Avinatan Hassidim, and Seth Lloyd. Quantum algorithm for linear systems of equations. *Physical review letters*, 103(15):150502, 2009.
- [6] Youngseok Kim, Andrew Eddins, Sajant Anand, Ken Xuan Wei, Ewout Van Den Berg, Sami Rosenblatt, Hasan Nayfeh, Yantao Wu, Michael Zaletel, Kristan Temme, et al. Evidence for the utility of quantum computing before fault tolerance. *Nature*, 618(7965):500–505, 2023.
- [7] Alberto Di Meglio, Karl Jansen, Ivano Tavernelli, Constantia Alexandrou, Srinivasan Arunachalam, Christian W Bauer, Kerstin Borrás, Stefano Carrazza, Arianna Crippa, Vincent Croft, et al. Quantum computing for high-energy physics: State of the art and challenges. *Prx quantum*, 5(3):037001, 2024.
- [8] Roland C Farrell, Marc Illa, Anthony N Ciavarella, and Martin J Savage. Quantum simulations of hadron dynamics in the schwinger model using 112 qubits. *Physical Review D*, 109(11):114510, 2024.
- [9] Dmitry A Abanin, Rajeev Acharya, Laleh Aghababaie-Beni, Georg Aigeldinger, Ashok Ajoy, Ross Alcaraz, Igor Aleiner, Trond I Andersen, Markus Ansmann, Frank Arute, et al. Observation of constructive interference at the edge of quantum ergodicity. *Nature*, 646(8086):825–830, 2025.
- [10] Laurin E Fischer, Matea Leahy, Andrew Eddins, Nathan Keenan, Davide Ferracin, Matteo AC Rossi, Youngseok Kim, Andre He, Francesca Pietracaprina, Boris Sokolov, et al. Dynamical simulations of many-body quantum chaos on a quantum computer. *Nature Physics*, pages 1–6, 2026.

- [11] Abhinav Kandala, Antonio Mezzacapo, Kristan Temme, Maika Takita, Markus Brink, Jerry M Chow, and Jay M Gambetta. Hardware-efficient variational quantum eigensolver for small molecules and quantum magnets. *nature*, 549(7671):242–246, 2017.
- [12] Sam McArdle, Suguru Endo, Alán Aspuru-Guzik, Simon C Benjamin, and Xiao Yuan. Quantum computational chemistry. *Reviews of Modern Physics*, 92(1):015003, 2020.
- [13] Bela Bauer, Sergey Bravyi, Mario Motta, and Garnet Kin-Lic Chan. Quantum algorithms for quantum chemistry and quantum materials science. *Chemical reviews*, 120(22):12685–12717, 2020.
- [14] Vera von Burg, Guang Hao Low, Thomas Häner, Damian S Steiger, Markus Reiher, Martin Roetteler, and Matthias Troyer. Quantum computing enhanced computational catalysis. *Physical Review Research*, 3(3):033055, 2021.
- [15] Weitang Li, Zhi Yin, Xiaoran Li, Dongqiang Ma, Shuang Yi, Zhenxing Zhang, Chenji Zou, Kunliang Bu, Maochun Dai, Jie Yue, et al. A hybrid quantum computing pipeline for real world drug discovery. *Scientific Reports*, 14(1):16942, 2024.
- [16] Danil Kaliakin, Akhil Shajan, Fangchun Liang, and Kenneth M Merz Jr. Implicit solvent sample-based quantum diagonalization. *The Journal of Physical Chemistry B*, 129(23):5788–5796, 2025.
- [17] Nikolaj Moll, Panagiotis Barkoutsos, Lev S Bishop, Jerry M Chow, Andrew Cross, Daniel J Egger, Stefan Filipp, Andreas Fuhrer, Jay M Gambetta, Marc Ganzhorn, et al. Quantum optimization using variational algorithms on near-term quantum devices. *Quantum Science and Technology*, 3(3):030503, 2018.
- [18] Earl Campbell, Ankur Khurana, and Ashley Montanaro. Applying quantum algorithms to constraint satisfaction problems. *Quantum*, 3:167, 2019.
- [19] Ashley Montanaro. Quantum speedup of branch-and-bound algorithms. *Physical Review Research*, 2(1):013056, 2020.
- [20] Daniel J Egger, Jakub Mareček, and Stefan Woerner. Warm-starting quantum optimization. *Quantum*, 5:479, 2021.
- [21] Amira Abbas, Andris Ambainis, Brandon Augustino, Andreas Bärttschi, Harry Buhrman, Carleton Coffrin, Giorgio Cortiana, Vedran Dunjko, Daniel J Egger, Bruce G Elmegreen, et al. Challenges and opportunities in quantum optimization. *Nature Reviews Physics*, 6(12):718–735, 2024.
- [22] Sebastián V Romero, Anne-Maria Visuri, Alejandro Gomez Cadavid, Anton Simen, Enrique Solano, and Narendra N Hegade. Bias-field digitized counterdiabatic quantum algorithm for higher-order binary optimization. *Communications Physics*, 8(1):348, 2025.
- [23] Ayse Kotil, Elijah Pelofske, Stephanie Riedmüller, Daniel J Egger, Stephan Eidenbenz, Thorsten Koch, and Stefan Woerner. Quantum approximate multi-objective optimization. *Nature Computational Science*, pages 1–10, 2025.
- [24] Sabina Drăgoi, Alberto Baiardi, and Daniel J Egger. Approximate quadratization of high-order hamiltonians for combinatorial quantum optimization. *Physical Review Research*, 8(2):023159, 2026.
- [25] Jacob Biamonte, Peter Wittek, Nicola Pancotti, Patrick Rebentrost, Nathan Wiebe, and Seth Lloyd. Quantum machine learning. *Nature*, 549(7671):195–202, 2017.
- [26] Nana Liu and Patrick Rebentrost. Quantum machine learning for quantum anomaly detection. *Physical Review A*, 97(4):042315, 2018.
- [27] Iris Cong, Soonwon Choi, and Mikhail D Lukin. Quantum convolutional neural networks. *Nature Physics*, 15(12):1273–1278, 2019.
- [28] Vojtěch Havlíček, Antonio D Córcoles, Kristan Temme, Aram W Harrow, Abhinav Kandala, Jerry M Chow, and Jay M Gambetta. Supervised learning with quantum-enhanced feature spaces. *Nature*, 567(7747):209–212, 2019.
- [29] Maria Schuld and Nathan Killoran. Quantum machine learning in feature hilbert spaces. *Physical review letters*, 122(4):040504, 2019.
- [30] Hsin-Yuan Huang, Michael Broughton, Masoud Mohseni, Ryan Babbush, Sergio Boixo, Hartmut Neven, and Jarrod R McClean. Power of data in quantum machine learning. *Nature communications*, 12(1):2631, 2021.
- [31] Marco Cerezo, Guillaume Verdon, Hsin-Yuan Huang, Lukasz Cincio, and Patrick J Coles. Challenges and opportunities in quantum machine learning. *Nature computational science*, 2(9):567–576, 2022.
- [32] Jennifer R Glick, Tanvi P Gujarati, Antonio D Corcoles, Youngseok Kim, Abhinav Kandala, Jay M Gambetta, and Kristan Temme. Covariant quantum kernels for data with group structure. *Nature Physics*, 20(3):479–483, 2024.
- [33] Stefan Woerner and Daniel J Egger. Quantum risk analysis. *npj Quantum Information*, 5(1):15, 2019.

- [34] Daniel J Egger, Claudio Gambella, Jakub Marecek, Scott McFaddin, Martin Mevissen, Rudy Raymond, Andrea Simonetto, Stefan Woerner, and Elena Yndurain. Quantum computing for finance: State-of-the-art and future prospects. *IEEE Transactions on Quantum Engineering*, 1:1–24, 2020.
- [35] Nikitas Stamatopoulos, Daniel J Egger, Yue Sun, Christa Zoufal, Raban Iten, Ning Shen, and Stefan Woerner. Option pricing using quantum computers. *Quantum*, 4:291, 2020.
- [36] Daniel J Egger, Ricardo García Gutiérrez, Jordi Cahué Mestre, and Stefan Woerner. Credit risk analysis using quantum computers. *IEEE transactions on computers*, 70(12):2136–2145, 2020.
- [37] J.V.S Scursulim, G.M. Langeloh, V. L. Beltran, and et al. Multiclass portfolio optimization via variational quantum eigensolver with dicke state ansatz. *Scientific Reports*, 16(6208), 2026.
- [38] John Preskill. Quantum computing in the nisq era and beyond. *Quantum*, 2:79, 2018.
- [39] Abhinav Kandala, Kristan Temme, Antonio D Corcoles, Antonio Mezzacapo, Jerry M Chow, and Jay M Gambetta. Extending the computational reach of a noisy superconducting quantum processor. *arXiv preprint arXiv:1805.04492*, 2018.
- [40] Tudor Giurgica-Tiron, Yousef Hindy, Ryan LaRose, Andrea Mari, and William J Zeng. Digital zero noise extrapolation for quantum error mitigation. In *2020 IEEE international conference on quantum computing and engineering (QCE)*, pages 306–316. IEEE, 2020.
- [41] Paul D Nation, Hwajung Kang, Neereja Sundaresan, and Jay M Gambetta. Scalable mitigation of measurement errors on quantum computers. *PRX Quantum*, 2(4):040326, 2021.
- [42] Ewout Van Den Berg, Zlatko K Mineev, and Kristan Temme. Model-free readout-error mitigation for quantum expectation values. *Physical Review A*, 105(3):032620, 2022.
- [43] Sergei Filippov, Matea Leahy, Matteo AC Rossi, and Guillermo García-Pérez. Scalable tensor-network error mitigation for near-term quantum computing. *arXiv preprint arXiv:2307.11740*, 2023.
- [44] Ewout Van Den Berg, Zlatko K Mineev, Abhinav Kandala, and Kristan Temme. Probabilistic error cancellation with sparse pauli–lindblad models on noisy quantum processors. *Nature physics*, 19(8):1116–1121, 2023.
- [45] Youngseok Kim, Christopher J Wood, Theodore J Yoder, Seth T Merkel, Jay M Gambetta, Kristan Temme, and Abhinav Kandala. Scalable error mitigation for noisy quantum circuits produces competitive expectation values. *Nature Physics*, 19(5):752–759, 2023.
- [46] Riddhi S Gupta, Ewout Van Den Berg, Maika Takita, Diego Riste, Kristan Temme, and Abhinav Kandala. Probabilistic error cancellation for dynamic quantum circuits. *Physical Review A*, 109(6):062617, 2024.
- [47] Andrew Eddins, Minh C Tran, and Patrick Rall. Lightcone shading for classically accelerated quantum error mitigation. *arXiv preprint arXiv:2409.04401*, 2024.
- [48] Bryce Fuller, Minh C Tran, Danylo Lykov, Caleb Johnson, Max Rossmannek, Ken Xuan Wei, Andre He, Youngseok Kim, DinhDuy Vu, Kunal Sharma, et al. Improved quantum computation using operator backpropagation. *npj Quantum Information*, 2026.
- [49] Gideon Bass, Maxwell Henderson, Joshua Heath, and Joseph Dulny III. Optimizing the optimizer: decomposition techniques for quantum annealing. *Quantum Machine Intelligence*, 3(1):10, 2021.
- [50] Marco Cerezo, Andrew Arrasmith, Ryan Babbush, Simon C Benjamin, Suguru Endo, Keisuke Fujii, Jarrod R McClean, Kosuke Mitarai, Xiao Yuan, Lukasz Cincio, et al. Variational quantum algorithms. *Nature Reviews Physics*, 3(9):625–644, 2021.
- [51] Alberto Peruzzo, Jarrod McClean, Peter Shadbolt, Man-Hong Yung, Xiao-Qi Zhou, Peter J Love, Alán Aspuru-Guzik, and Jeremy L O’Brien. A variational eigenvalue solver on a photonic quantum processor. *Nature communications*, 5(1):4213, 2014.
- [52] Edward Farhi, Jeffrey Goldstone, and Sam Gutmann. A quantum approximate optimization algorithm. *arXiv preprint arXiv:1411.4028*, 2014.
- [53] Zoë Holmes, Kunal Sharma, Marco Cerezo, and Patrick J Coles. Connecting ansatz expressibility to gradient magnitudes and barren plateaus. *PRX quantum*, 3(1):010313, 2022.
- [54] Samson Wang, Enrico Fontana, Marco Cerezo, Kunal Sharma, Akira Sone, Lukasz Cincio, and Patrick J Coles. Noise-induced barren plateaus in variational quantum algorithms. *Nature communications*, 12(1):6961, 2021.
- [55] Martin Larocca, Supanut Thanasilp, Samson Wang, Kunal Sharma, Jacob Biamonte, Patrick J Coles, Lukasz Cincio, Jarrod R McClean, Zoë Holmes, and Marco Cerezo. Barren plateaus in variational quantum computing. *Nature Reviews Physics*, 7(4):174–189, 2025.

- [56] Giuseppe Scriva, Nikita Astrakhantsev, Sebastiano Pilati, and Guglielmo Mazzola. Challenges of variational quantum optimization with measurement shot noise. *Physical Review A*, 109(3):032408, 2024.
- [57] Lennart Bittel and Martin Kliesch. Training variational quantum algorithms is np-hard. *Physical review letters*, 127(12):120502, 2021.
- [58] Heinz-Peter Breuer and Francesco Petruccione. *The theory of open quantum systems*. OUP Oxford, 2002.
- [59] Michael A Nielsen and Isaac L Chuang. *Quantum computation and quantum information*. Cambridge university press, 2010.
- [60] Marco Cerezo, Kunal Sharma, Andrew Arrasmith, and Patrick J Coles. Variational quantum state eigensolver. *npj Quantum Information*, 8(1):113, 2022.
- [61] Huanfeng Zhao, Peng Zhang, and Tzu-Chieh Wei. A universal variational quantum eigensolver for non-hermitian systems. *Scientific Reports*, 13(1):22313, 2023.
- [62] Zhong-Xia Shang. Hermitian-preserving ansatz and variational open quantum eigensolver. *Physical Review A*, 109(6):062608, 2024.
- [63] Giuseppe Clemente. Mixed state variational quantum eigensolver for the estimation of expectation values at finite temperature. *arXiv preprint arXiv:2401.17194*, 2024.
- [64] Sascha Mücke, Raoul Heese, Sabine Müller, Moritz Wolter, and Nico Piatkowski. Feature selection on quantum computers. *Quantum Machine Intelligence*, 5(1):11, 2023.
- [65] Lucas Leclerc, Luis Ortiz-Gutiérrez, Sebastián Grijalva, Boris Albrecht, Julia RK Cline, Vincent E Elfving, Adrien Signoles, Loïc Henriët, Gianni Del Bimbo, Usman Ayub Sheikh, et al. Financial risk management on a neutral atom quantum processor. *Physical Review Research*, 5(4):043117, 2023.
- [66] Harry Markowitz. Portfolio selection. *The Journal of Finance*, 7(1):77–91, 1952.
- [67] Fred Glover, Gary Kochenberger, Rick Hennig, and Yu Du. Quantum bridge analytics i: a tutorial on formulating and using qubo models. *Annals of Operations Research*, 314(1):141–183, 2022.
- [68] Andrew Lucas. Ising formulations of many np problems. *Frontiers in physics*, 2:74887, 2014.
- [69] David J Griffiths and Darrell F Schroeter. *Introduction to quantum mechanics*. Cambridge university press, 2018.
- [70] Barry M Garraway. The dicke model in quantum optics: Dicke model revisited. *Philosophical Transactions of the Royal Society A: Mathematical, Physical and Engineering Sciences*, 369(1939):1137–1155, 2011.
- [71] Robert Prevedel, Gunther Cronenberg, Mark S Tame, Mauro Paternostro, Philip Walther, Mu-Seong Kim, and Anton Zeilinger. Experimental realization of dicke states of up to six qubits for multiparty quantum networking. *Physical review letters*, 103(2):020503, 2009.
- [72] Géza Tóth. Multipartite entanglement and high-precision metrology. *Physical Review A—Atomic, Molecular, and Optical Physics*, 85(2):022322, 2012.
- [73] Yingkai Ouyang. Permutation-invariant quantum coding for quantum deletion channels. In *2021 IEEE International Symposium on Information Theory (ISIT)*, pages 1499–1503. IEEE, 2021.
- [74] Yingkai Ouyang. Quantum storage in quantum ferromagnets. *Physical Review B*, 103(14):144417, 2021.
- [75] Minhyeok Kang, Jaehee Kim, William J Munro, Seungbeom Chin, and Joonsuk Huh. Heralded linear optical generation of dicke states. *New Journal of Physics*, 28(5):054501, 2026.
- [76] Shengbin Wang, Peng Wang, Guihui Li, Shubin Zhao, Dongyi Zhao, Jing Wang, Yuan Fang, Menghan Dou, Yongjian Gu, Yu-Chun Wu, et al. Variational quantum eigensolver with linear depth problem-inspired ansatz for solving portfolio optimization in finance. *Science China Information Sciences*, 68(8):180504, 2025.
- [77] Maximilian Schlosshauer. *Decoherence and the quantum-to-classical transition*. Springer, 2007.
- [78] Steven Weinberg. *Lectures on quantum mechanics*. Cambridge University Press, 2015.
- [79] Alexander V Grayver and Alexey V Kuvshinov. Exploring equivalence domain in nonlinear inverse problems using covariance matrix adaption evolution strategy (cmaes) and random sampling. *Geophysical Journal International*, 205(2):971–987, 2016.
- [80] Michael JD Powell. A direct search optimization method that models the objective and constraint functions by linear interpolation. In *Advances in optimization and numerical analysis*, pages 51–67. Springer, 1994.
- [81] Gadi Aleksandrowicz, Thomas Alexander, Panagiotis Barkoutsos, Luciano Bello, Yael Ben-Haim, David Bucher, Francisco Jose Cabrera-Hernández, Jorge Carballo-Franquis, Adrian Chen, Chun-Fu Chen, et al. Qiskit: An open-source framework for quantum computing. *Zenodo*, 2019.
- [82] Philip Krantz, Morten Kjaergaard, Fei Yan, Terry P Orlando, Simon Gustavsson, and William D Oliver. A quantum engineer’s guide to superconducting qubits. *Applied physics reviews*, 6(2), 2019.

A Derivation of the Mixed-State VQE Objective Function

We derive here the simplified form of the VQE objective function 10 for combinatorial optimization problems whose Hamiltonian is diagonal in the computational basis, i.e. $H = \sum_{x \in \{0,1\}^n} E_x |x\rangle\langle x|$. The derivation exploits the linearity of the trace operation and the structure of the mixed Dicke state ansatz 9.

$$\begin{aligned}
\langle H \rangle &= \text{tr}(\sigma(\vec{\alpha}, \vec{\theta})H) \\
&= \text{tr} \left(\sum_k p_k(\vec{\alpha}) |D_k^n(\vec{\theta})\rangle \langle D_k^n(\vec{\theta})| \sum_{x \in \{0,1\}^n} E_x |x\rangle\langle x| \right) \\
&= \sum_k p_k(\vec{\alpha}) \sum_{x \in \{0,1\}^n} E_x \text{tr} \left(|D_k^n(\vec{\theta})\rangle \langle D_k^n(\vec{\theta})| x \rangle \langle x| \right) \\
&= \sum_k p_k(\vec{\alpha}) \sum_{x \in \{0,1\}^n} E_x |\langle x | D_k^n(\vec{\theta}) \rangle|^2 \\
&= \sum_k \sum_{\substack{x \in \{0,1\}^n \\ \text{hw}(x)=k}} p_k(\vec{\alpha}) |c_x(\vec{\theta})|^2 E_x \\
&= \sum_m \sigma_{mm}(\vec{\alpha}, \vec{\theta}) E_m
\end{aligned} \tag{23}$$

The final expression shows that the objective function reduces to a weighted sum of energies E_x with weights given by the diagonal elements $\sigma_{mm}(\vec{\alpha}, \vec{\theta}) = p_{\text{hw}(m)}(\vec{\alpha}) |c_m(\vec{\theta})|^2$, which correspond to the measurement outcome probabilities extracted directly from the quantum circuit.

B Effects of Finite Sampling on the Variational Optimization Landscape

In this appendix, we examine the effects of finite sampling on the variational optimization landscape, since in practice we have access only to samples from the probability distribution associated with the quantum state prepared by the circuit. The standard deviation of the expectation value of an operator O follows

$$\sigma_{\langle O \rangle} \propto \frac{1}{\sqrt{n_{\text{shots}}}}. \tag{24}$$

In the noiseless limit, this quantity satisfies

$$\lim_{n_{\text{shots}} \rightarrow \infty} \sigma_{\langle O \rangle} = 0, \tag{25}$$

corresponding to the regime where the complete probability distribution is recovered. Figure 5 illustrates the behavior of 24 as the number of shots increases, where the dashed line indicates the noiseless limit $\sigma_{\langle O \rangle} = 0$.

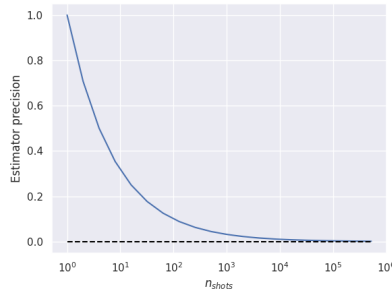


Figure 5: Estimator standard deviation $\sigma_{\langle O \rangle}$ as a function of n_{shots} illustrating the $1/\sqrt{n_{\text{shots}}}$ decay. The dashed line indicates the noiseless statevector limit, recovered as $n_{\text{shots}} \rightarrow \infty$.

In practice, we have access only to a finite sample of the probability distribution and must consider the effects of finite sampling on variational quantum algorithms. As illustrated in Figure 6, increasing the number of shots progressively smooths the optimization landscape — finite sampling introduces spurious local minima and produces a non-smooth

surface, imposing additional challenges for gradient-based optimizers. The choice of CMA-ES [79] and COBYLA [80] was motivated by these considerations. In order not to exceed the regime where these algorithms perform worse than random search with replacement [56], it is necessary to carefully balance the number of shots and iterations.

The surfaces in Figure 6 were generated by randomly selecting 3 assets with seed 42 to compose a portfolio optimization instance in which exactly one asset is selected, using the ansatz

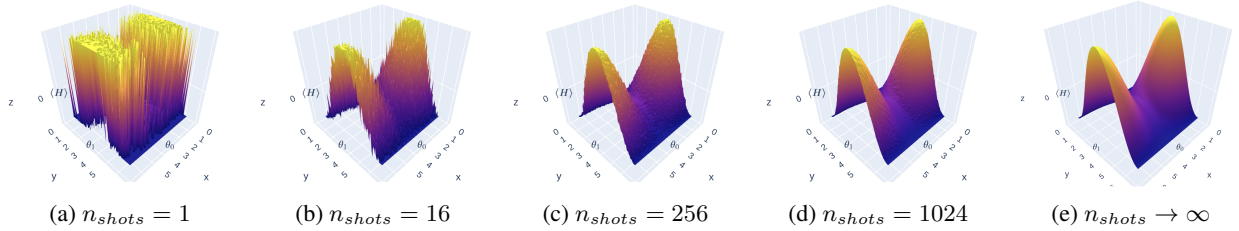


Figure 6: Energy landscape $\langle H \rangle$ as a function of the variational parameters θ_0 and θ_1 for increasing number of measurement shots. As the number of shots increases, the landscape progressively smooths toward the noiseless statevector limit ($n_{shots} \rightarrow \infty$), illustrating the impact of finite sampling noise on the optimization surface.

C Hardware experiments

In order to assess the performance of the proposed ansatz on current noisy quantum hardware, we performed state preparation experiments and evaluated the Hamiltonian expectation value for each scenario. For these experiments, we selected the simulation run in which the CMA-ES optimizer yielded parameter vectors maximizing the sampling probability of the target bitstring x^* . In all experiments, the number of shots was set to 4096. Experiments were executed using the Sampler and Estimator primitives on the devices `ibm_kingston`, `ibm_fez`, and `ibm_marrakesh`. The calibration data for all devices used in this study are available in the project repository (see Data Availability statement).

The similarity between the probability distributions obtained from simulation and hardware runs was evaluated using two complementary metrics. The first is the Kullback-Leibler divergence, defined as

$$D_{KL}(P||Q) = \sum_{x \in \mathcal{X}} P(x) \log \frac{P(x)}{Q(x)}, \quad (26)$$

where P and Q are probabilities distributions. Note that $D_{KL}(P||Q) = 0$ if and only if $P = Q$, and $D_{KL}(P||Q) > 0$ indicates a discrepancy between the distributions, with larger values corresponding to greater divergence. It is also important to note that (26) is asymmetric, i.e. $D_{KL}(P||Q) \neq D_{KL}(Q||P)$ in general. The second metric is the Hellinger fidelity [59], defined as

$$F(P, Q) = \left(\sum_i \sqrt{p_i q_i} \right)^2, \quad (27)$$

where $0 \leq F(P, Q) \leq 1$. A value of $F(P, Q) = 1$ indicates that $P = Q$, while $F(P, Q) = 0$ indicates that the distributions have disjoint support. Intermediate values reflect the degree of overlap between the two distributions.

The results obtained through the Sampler and Estimator primitives are presented in Tables 1 and 2, respectively. The Sampler results reveal low fidelity and high KL divergence values in most cases, indicating that hardware noise significantly distorted the prepared distributions relative to the simulation reference. The Estimator results show relative errors of approximately 50% across all QPUs and scenarios, confirming that the cumulative effect of two-qubit gate noise substantially degraded the objective function estimates. These results highlight the need for more advanced error mitigation techniques and circuit transpilation optimizations before the proposed ansatz can yield reliable results on current NISQ hardware.

Table 1: Hardware experiment results for each QPU and scenario, reporting KL divergence, fidelity, and target bitstring probability.

QPU	Scenario	KL Divergence	Fidelity	Target Probability
ibm_kingston	I	5.540569	0.008845	0.000488
	II	0.452282	0.000940	0.000000
	III	6.164810	0.003155	0.000732
ibm_fez	I	4.437095	0.008741	0.001953
	II	0.004935	0.000009	0.000000
	III	7.079446	0.001906	0.000244
ibm_marrakesh	I	0.396861	0.002275	0.000000
	II	0.358606	0.000220	0.000000
	III	6.500446	0.002231	0.000488

Table 2: Objective function values and relative errors obtained on real quantum hardware for each QPU and scenario, where the relative error is defined as $|\text{obj_value} - \text{reference}|/|\text{reference}|$. The reference values correspond to the objective function values obtained in simulation experiments where the target bitstring x^* was the most probable outcome after training: -0.8352 , -0.8273 , and -2.0527 for Scenarios I, II, and III, respectively.

QPU	Scenario	Objective Value	Relative Error
ibm_kingston	Scenario I	-0.423282	0.493171
	Scenario II	-0.427963	0.482729
	Scenario III	-0.980868	0.522153
ibm_fez	Scenario I	-0.412210	0.506428
	Scenario II	-0.424199	0.487278
	Scenario III	-0.982028	0.521587
ibm_marrakesh	Scenario I	-0.437973	0.475581
	Scenario II	-0.421351	0.490721
	Scenario III	-0.968446	0.528204